

# Rapid preparation of tritium breeder material $\text{Li}_2\text{TiO}_3$ pebbles by thermal plasma



Hailong Zhu<sup>a,\*</sup>, Honghui Tong<sup>b</sup>, Changming Cheng<sup>b</sup>

<sup>a</sup> College of Physics and Electronics Engineering, Shanxi University, Taiyuan 030006, China

<sup>b</sup> Southwestern Institute of Physics, Chengdu 610041, China

## ARTICLE INFO

### Article history:

Available online 17 May 2016

## ABSTRACT

A route to obtain tritium breeder material  $\text{Li}_2\text{TiO}_3$  pebbles in one step was investigated using a direct-current (DC) thermal plasma system. For this purpose, irregular and agglomerate powders were used as raw powders which were injected into DC thermal plasma torch with a plasma power level of  $\sim 18$  kW. The morphology, particles size distribution and phase change of the prepared  $\text{Li}_2\text{TiO}_3$  pebbles were characterized by field-emission scanning electron microscope and X-ray diffraction (XRD). The results showed that prepared  $\text{Li}_2\text{TiO}_3$  pebbles presented excellent spherical degree with average size about  $100\ \mu\text{m}$  and the spheroidization rate was close to 100%. The XRD patterns demonstrated that higher degree of crystallinity of  $\text{Li}_2\text{TiO}_3$  pebbles could be obtained by thermal plasma processed. Formation mechanism of  $\text{Li}_2\text{TiO}_3$  pebbles in DC thermal plasma system was discussed.

© 2016 The Authors. Published by Elsevier Ltd.

This is an open access article under the CC BY-NC-ND license (<http://creativecommons.org/licenses/by-nc-nd/4.0/>).

## 1. Introduction

As a key Li-ceramics material,  $\text{Li}_2\text{TiO}_3$  has been considered as candidate for tritium breeder materials in ITER test blanket module, because of its reasonable lithium atom density, low activation, excellent chemical stability, good compatibility with structural materials and good tritium release characteristics at low temperature [1–4]. This tritium breeder material can be solidified into column, circular or spherical shape. Among these, spherical  $\text{Li}_2\text{TiO}_3$  are considered as the preferred materials due to the large specific surface, more channels between the pebbles, good permeability which is conducive to the diffusion and release of tritium.

Some methods for the preparation of  $\text{Li}_2\text{TiO}_3$  pebbles have been proposed in the past two decades, such as extrusion-spheronisation-sintering [5], sol-gel process [6], wet process [7,8], and melting granulation method [9]. Although these methods have been adopted to prepare  $\text{Li}_2\text{TiO}_3$  pebbles with good degree of sphericity and higher yields, there are still some difficulties during the process of preparation, such as long reaction time, complex procedure, tough conditions, even bringing to pollution, such as waste water and toxic gases.

In recent years, some people reported the preparation method of spherical powder by thermal plasma, including a variety of re-

fractory metallic and ceramic powder, such as nickel [10], tungsten [11], alumina [12], silicon carbide [13] and so forth. This preparation method of spherical powder is based on high processing temperature in plasma core area (up to  $1.0 \times 10^4$  K), and fast quenching rate ( $\sim 10^5\text{--}10^6$  Ks<sup>−1</sup>) at the plasma tail [14,15]. Any powders which are injected into the thermal plasma are heated up and melted down immediately, and then become spheres due to surface tension; the melted droplets solidify into spherical particles due to rapidly quenching when they spurt out of the plasma. The sphericity and flowability, and mechanical properties of prepared spherical powder have been significantly improved. In addition, the high-light advantage of this method is one-step-preparation without any additional pollution in the preparation process. In particular, the preparation of tritium breeder material  $\text{Li}_2\text{TiO}_3$  pebbles by thermal plasma has not been reported.

Thermal plasma can be generated by various methods of discharges, i.e. radio frequency (RF) inductively coupled discharge, and DC arc discharge. Although RF inductively coupled thermal plasma has advantages, such as absence of electrode pollution, lower velocity resulting in long residence time of powder in plasma, the flow instability and lower electric-thermal conversion efficiency limit it to be widely used. DC thermal plasma has excellent flow stability and higher electric-thermal conversion efficiency which can reduce the preparation cost effectively.

In this work, the application of nitrogen plasma for preparation  $\text{Li}_2\text{TiO}_3$  pebbles is presented firstly. The ultra-fine and

\* Corresponding author.

E-mail address: [zhuhl@sxu.edu.cn](mailto:zhuhl@sxu.edu.cn) (H. Zhu).

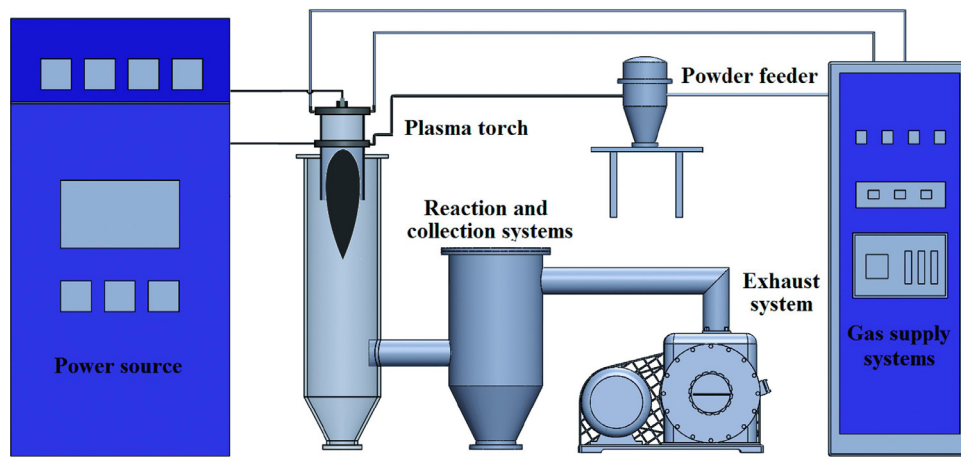


Fig. 1. Schematic illustration of the experimental setup.

agglomerated  $\text{Li}_2\text{TiO}_3$  powder as raw materials is introduced into the reactor and mixed with thermal plasma jet. The morphology and crystallography of prepared  $\text{Li}_2\text{TiO}_3$  pebbles are characterized. The forming mechanism of  $\text{Li}_2\text{TiO}_3$  pebbles is discussed in the end.

## 2. Experimental setup and methodology

The experiment aiming at preparing  $\text{Li}_2\text{TiO}_3$  pebbles was performed by DC thermal plasma operating with a homemade plasma torch. The plasma torch was energized by a DC power supply with a maximum output capacity of 50 kW, and nitrogen was used as the plasma gas. The plasma working gas introduced between the anode and trigger electrode is used to produce a stable plasma, the protective nitrogen gas injected between cathode and trigger electrode is used as a shroud gas to protect the cerium-tungsten cathode, and the role of the carrier gas is to transport the raw powder into the plasma torch. The raw powder was injected into the plasma torch using a homemade rotary powder feeder with the nitrogen carrier gas. A tubular reaction chamber with cooling water outside was closely connected to the plasma torch. Followed the reaction chamber, there is a powder collection chamber connected with a two-stage water-ring vacuum pump which was used to maintain a negative pressure. The gas supply systems were used continuously to provide nitrogen for plasma and powder feeder. A schematic description of the experimental setup is shown in Fig. 1.

The experiment is conducted as follows. Firstly, a small amount of nitrogen gas was injected into the plasma torch in order to ignite the plasma by applying a high-frequency voltage, then increase the input power and gas flow rate to maintain stable plasma. At this time, the plasma temperature is higher than the melting temperature of  $\text{Li}_2\text{TiO}_3$  material and the length of plasma flow is about 240 mm. Next, the raw powder was delivered to high temperature zone of plasma through the feeding mouth located between the anode and trigger electrode using the carrier gas. The injected powder will be heated up, melted down and even a small part of particles were vaporized when they flew into the high temperature region of the plasma torch, and the melted droplets would be quenched and solidified into spherical pebbles under the effect of surface tension when they spurt out of the plasma region. Finally, prepared  $\text{Li}_2\text{TiO}_3$  pebbles were collected from the bottom of the reaction and collection chamber. During the operation, the plasma power was 18 kW, calculated from the product of DC arc voltage (180 V) and the arc electric current (100 A). The plasma working gas, protective gas and carrier gas was supplied at the flow rate of 1.2, 3.0, and  $0.6 \text{ m}^3/\text{h}$ , respectively. The flow rate of the raw powder was controlled at  $10.0 \text{ g}/\text{min}$ .

Morphology and phase of the prepared samples was characterized by field-emission scanning electron microscope (FE-SEM, Model S-4800, Hitachi, Tokyo, Japan) and X-ray diffraction (XRD, X'pert Pro MPD, Philips, Netherlands), respectively. The size distribution of the  $\text{Li}_2\text{TiO}_3$  pebbles was subsequently determined from the FE-SEM micrographs on an image analyzer, with 350 pebbles counted in each batch.

The d50 value for each batch of  $\text{Li}_2\text{TiO}_3$  pebbles, that is the pebble size at the cumulative fraction of 50%, was used to denote the average pebble size, which was proposed by J-G Li [16].

## 3. Results and discussion

### 3.1. Morphology

The FE-SEM in Fig. 2(a) shows the morphology of raw  $\text{Li}_2\text{TiO}_3$  powders at different magnifications in this work. It is clearly seen that the raw powders are ultra-fine particles without any liquidity. In magnification image Fig. 2(b), it can be seen that the raw powder are very fine, irregular and easy to agglomerate. After processed by plasma, spherical  $\text{Li}_2\text{TiO}_3$  pebbles are formed and the FE-SEM image is shown in Fig. 3(a). It demonstrates that the prepared  $\text{Li}_2\text{TiO}_3$  pebbles present excellent spherical degree and spheroidization rate close to 100%, which is better than that achieved using the wet chemistry method [7]. This indicated that the raw  $\text{Li}_2\text{TiO}_3$  powders are melted completely through absorbed plasma energy at the feed rate of  $10 \text{ g}/\text{min}$ . The experiment found that at increased feed rate, some particles will not be sufficiently melted to become spheroidized and remain irregularly shaped. From magnification of  $\times 1000$  of Fig. 3(b), it can be seen that the  $\text{Li}_2\text{TiO}_3$  pebbles are composed of many small particles. Under the action of plasma flow, melted or partly melted droplets collide with each other, some of them even bond together, and then grow into larger droplets; finally the droplets are solidified and stuck to a larger particles. The same phenomenon was found in spheroidization of alumina [17,18].

Fig. 4 presents the energy dispersive spectrometer (EDS) spectrum of raw and prepared  $\text{Li}_2\text{TiO}_3$  pebbles. It shows that the powders almost exclusively composed of titanium and oxygen which the atomic ratio is close to 1:3, and there are no significant changes in weight and atomicity before and after plasma treatment. However, the EDS of the matrix could not show the presence of lithium because of its light weight. In addition, a traces of Al impurity were found in the EDS analysis of  $\text{Li}_2\text{TiO}_3$  pebbles. As shown in Fig 4(a), this Al impurity should be mainly introduced by

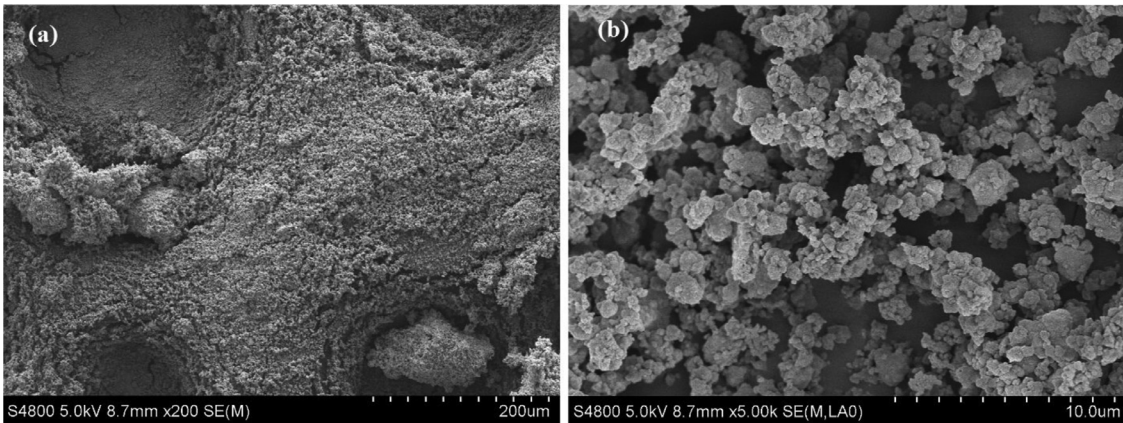


Fig. 2. FE-SEM image of raw powder: (a) magnification of  $\times 200$ , (b) magnification of  $\times 5000$ .

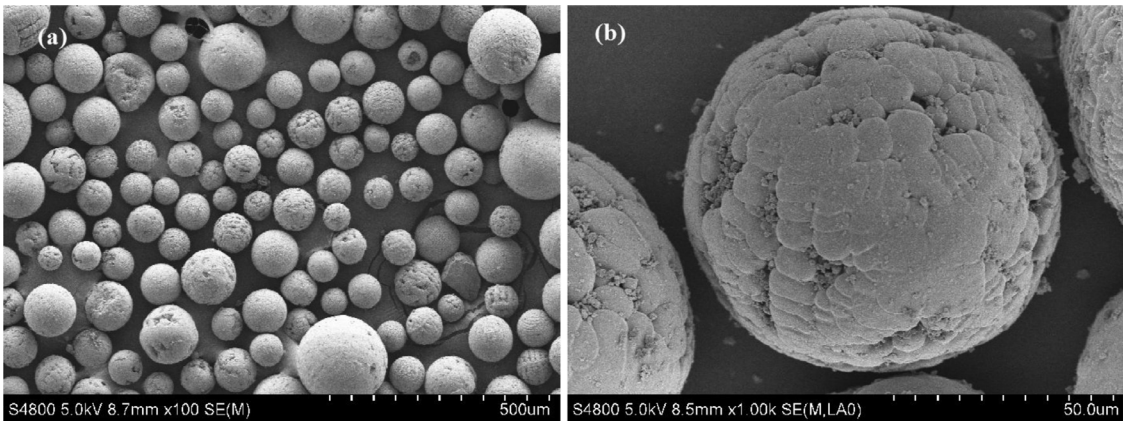


Fig. 3. FE-SEM image of prepared  $\text{Li}_2\text{TiO}_3$  pebbles: (a) magnification of  $\times 100$ , (b) magnification of  $\times 1000$ .

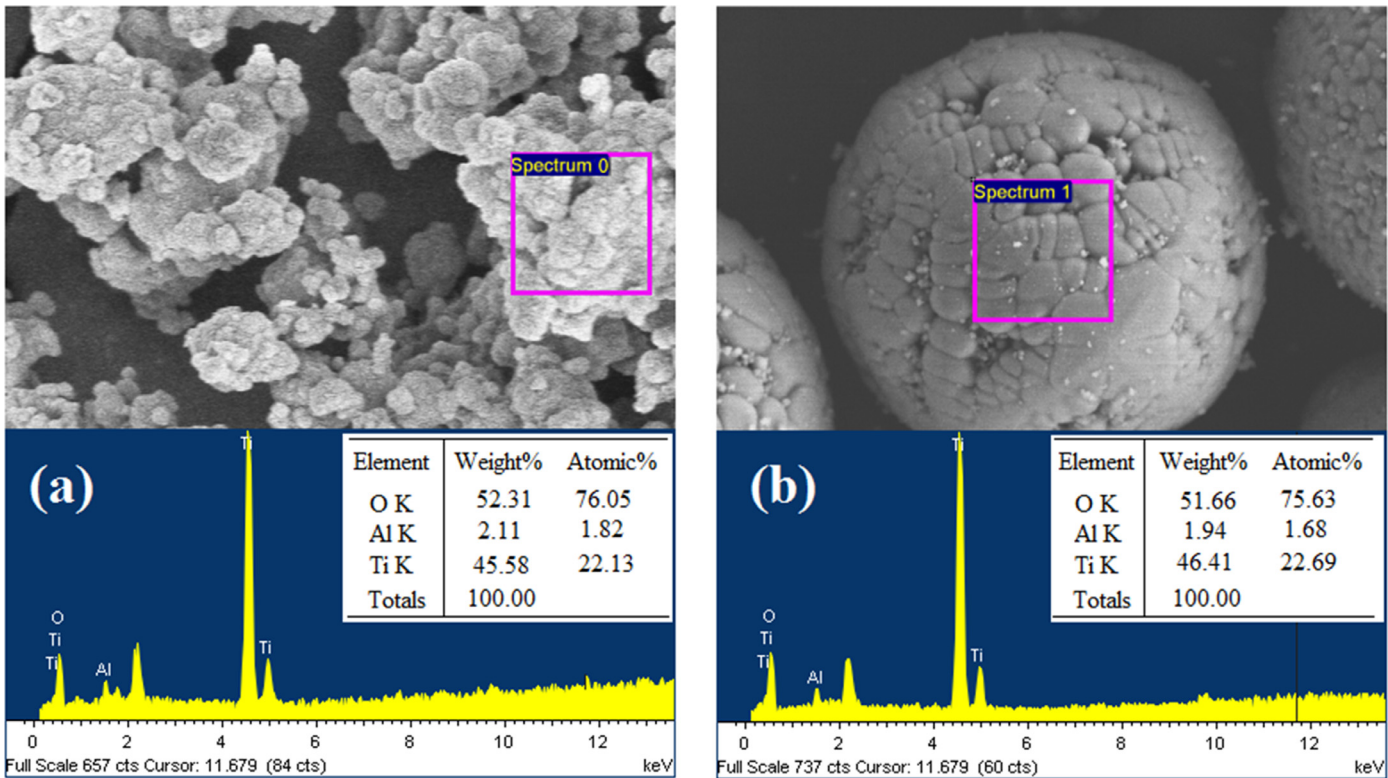


Fig. 4. EDS analysis of raw powders and prepared  $\text{Li}_2\text{TiO}_3$  pebbles.



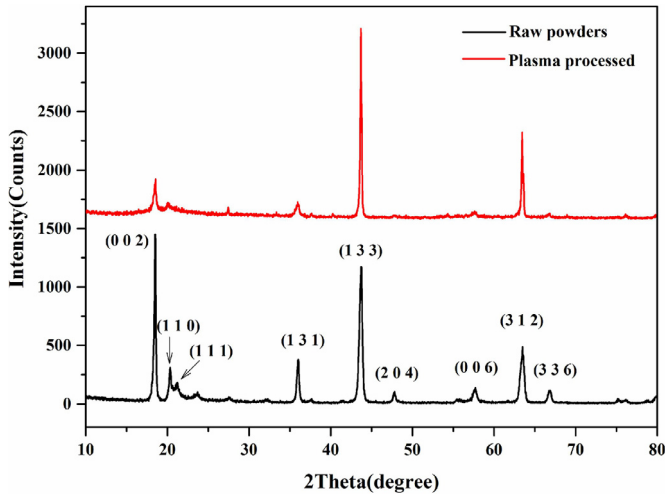


Fig. 5. the XRD patterns of  $\text{Li}_2\text{TiO}_3$  powder before and after thermal plasma processing.

raw powder. This phenomenon was well consistent with the reported results [19,20].

### 3.2. Crystallography

In order to ascertain the phases present and phase change taking place during the plasma processing, the X-ray pattern of the raw powder and the prepared  $\text{Li}_2\text{TiO}_3$  pebbles are exhibited in Fig. 5. The characteristic peaks of raw powder at  $2\theta$  are about  $18.0469^\circ$ ,  $43.582^\circ$ ,  $63.212^\circ$ , corresponding with  $d$  value are 4.8 Å, 2.075 Å, 21.4698 Å, respectively. All the sharp diffraction peaks can be indexed to monoclinic structured  $\text{Li}_2\text{TiO}_3$  and found to be well matching with JCPDC 33-0831. This phase is mainly from the  $\text{Li}_2\text{TiO}_3$  powder that was calcined at  $800^\circ\text{C}$ . After thermal plasma processing, the intensity of diffraction peaks reduces significantly at  $2\theta = 18.0469^\circ$  and enhances at  $43.582^\circ$ . These changes indicated that the preferential growth direction of this crystal is along the (1 3 3) direction by thermal plasma processing. The phase change is closely related to plasma temperature and the residence time of powder particles in plasma. Moreover, the full-width at half maximum (FWHM) of the (1 3 3) peak orientation of the XRD pattern of prepared  $\text{Li}_2\text{TiO}_3$  pebbles was narrower than that of raw powder. This indicated that a higher degree of crystallinity can be obtained by thermal plasma processed, and this method can improve effectively the quality of the materials by controlling the plasma parameters.

### 3.3. Size distributions

To investigate the variations in the particle size after the plasma spheroidization, the particle size distribution was analyzed by image analyzer software with 350 particles counted in a FE-SEM image. A comparison diagram for the size distribution of the samples before and after the spheroidization is shown in Fig. 6. It revealed that the raw material is the agglomerated sub-micron powder and the prepared  $\text{Li}_2\text{TiO}_3$  pebbles are mainly distributed in the  $50 \sim 250 \mu\text{m}$ , and the average size of the particles is about  $100 \mu\text{m}$ . The particle size has changed dramatically, which showed that  $D_{50}$  value changed from 0.54 to  $100 \mu\text{m}$ . This is consistent with our expectation that agglomerated sub-micron particles grow into spherical pebbles after plasma spheroidization. However, compared to the aforementioned method, the disadvantage of preparation of  $\text{Li}_2\text{TiO}_3$  pebbles by thermal plasma method is the wider particle size distribution and that the particles size is difficult to be controlled.

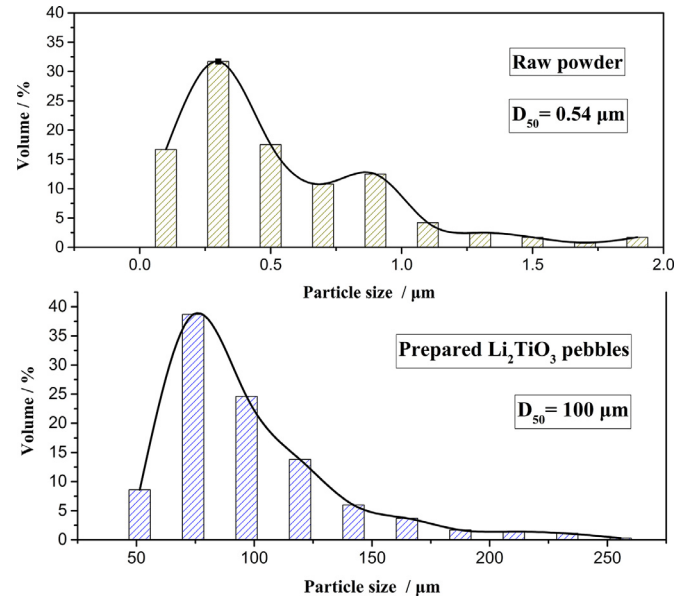


Fig. 6. The size distributions of raw powders and prepared  $\text{Li}_2\text{TiO}_3$  pebbles.

### 3.4. The formation process and key factors on preparation of $\text{Li}_2\text{TiO}_3$ pebbles

Based on the morphology and phase change of  $\text{Li}_2\text{TiO}_3$  pebbles aforementioned, the possible formation process of spherical  $\text{Li}_2\text{TiO}_3$  pebbles in plasma can be described as follows: The raw  $\text{Li}_2\text{TiO}_3$  powder are directly injected into the center of the plasma discharge region where the temperature can be as high as  $1.0 \times 10^4 \text{ K}$  [14,15]. The raw  $\text{Li}_2\text{TiO}_3$  powders are melted or partly melted through absorbed plasma energy in virtue of high temperature of the thermal plasma. The melting status of the powder particles is essential for the formation of pebbles, however, not all particles can be melted completely in spite of the plasma temperature being much higher than the melting point (1808 K) of the particles. This is attributed to the higher plasma velocity resulting in shorter residence time of powder particles in the plasma.

For a given powder particle, the particles size, melting point, thermal conductivity being fixed, the melting status of the powder particles is only determined by plasma temperature and velocity, because the plasma temperature is related to the melting time of the powder particles, and the plasma velocity determines the residence time of the powder particles. The residence time can be approximated as  $t_r = 2S/v_p$ , where  $S$  is length of the zone where the plasma temperature exceeds the melting temperature of particle and  $v_p$  is the particle axial velocity. The residence time are estimated as  $2 \sim 4.8 \text{ ms}$  in this experiment. According to the literature [21] the melting time can be formulated as  $t_m = \frac{r_p^2}{6} \left( 1 + \frac{2k}{hr_p} \right) \frac{\rho L}{k(T_f - T_m)}$ , where  $h$  is the heat transfer coefficient,  $T_f$  is the plasma temperature,  $T_m$  is the melting temperature,  $r_p$  is the radius of the raw powder,  $L$  is the latent heat of fusion, and  $k$  is the thermal conductivity of powder. The melting time for  $\text{Li}_2\text{TiO}_3$  powder with radius of  $1.0 \mu\text{m}$  are estimated as 1.6 ms. If  $t_m \leq t_r$ , powder particles can be melted effectively, otherwise, it is not melted or only partially melted. For  $\text{Li}_2\text{TiO}_3$  powder with the average size of  $0.54 \mu\text{m}$ , the powder particles can be melted effectively in this experimental condition.

The melted and partly melted particles collide and adhere with each other under the action of high-speed plasma flow resulting in the growth into large particles. And then the surface of the larger particles cools down rapidly when they fly into the tail region of

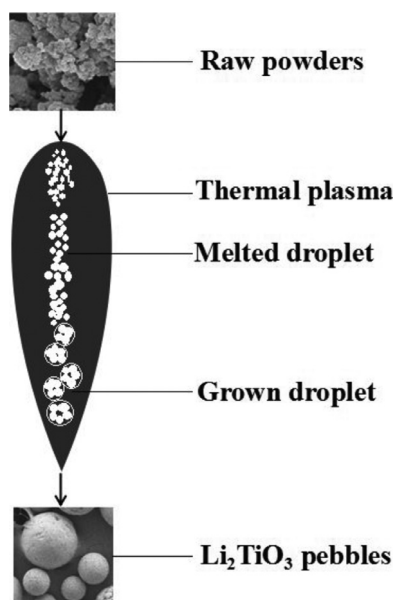


Fig. 7. Diagram of schematic of the formation process of  $\text{Li}_2\text{TiO}_3$  pebbles.

the plasma flame with rapidly quenching; in order to reduce surface energy of particles, the spherical form of  $\text{Li}_2\text{TiO}_3$  pebbles is obtained. Fig. 7 displays a process schematically depicting the formation process of spherical  $\text{Li}_2\text{TiO}_3$  pebbles in plasma.

The following are key factors in preparation of  $\text{Li}_2\text{TiO}_3$  pebbles based on our experimental findings:

- (1) Fast and complete melt of the raw  $\text{Li}_2\text{TiO}_3$  powder is a critical factor, therefore, improving the plasma power as much as possible is required in the DC thermal plasma system. However, the plasma power cannot be improved interminably considering electric energy consumptions in contact with the cost of preparation of  $\text{Li}_2\text{TiO}_3$  pebbles.
- (2) Gas-flow rate injected into plasma torch is another significant factor, because it determines the plasma velocity. Lower gas-flow rate, in other words, lower plasma velocity results in long residence time in the plasma discharge region which is favorable for melting of powder particles.
- (3) The preparation efficiency of  $\text{Li}_2\text{TiO}_3$  pebbles strongly depends on the feed rate of the starting material. We tend to believe that when the feed rate increases, the production efficiency of  $\text{Li}_2\text{TiO}_3$  pebbles should increase linearly. However, larger powder feed rate will lead to injected particles not melting completely in the plasma, and thus affects the quality and production efficiency of  $\text{Li}_2\text{TiO}_3$  pebbles. In our ex-

periment, the optimum range for the feed rates is identified to be within 8–18 g/min.

#### 4. Conclusion

In summary, a novel, economical and effective approach was developed to prepare  $\text{Li}_2\text{TiO}_3$  pebbles via rapidly melting and cooling process in DC arc thermal plasma system. The prepared  $\text{Li}_2\text{TiO}_3$  pebbles are in the range of 50–250  $\mu\text{m}$ , and presented a high degree of sphericity and crystallinity. The key in the formation process of pebbles lies in melting and cooling process of raw powder. The higher temperature is beneficial for the melting process of raw powder. Moreover, control of plasma speed is crucial for solidification of melted droplets. The effect of process parameters on the growth of  $\text{Li}_2\text{TiO}_3$  pebbles will be further discussed in the next work.

#### Acknowledgments

This work is supported by the National Natural Science Foundation of China (No. 11205050).

#### References

- [1] D. Mandal, M.R.K. Sheno, S.K. Ghosh, *Fusion Eng. Des.* 85 (2010) 819–823.
- [2] K. Omoto, T. Hashimoto, K. Sasaki, T. Terai, T. Hoshino, M. Yashima, *J. Nucl. Mater.* 417 (2011) 692–695.
- [3] M. Hong, Y. Zhang, M. Xiang, Y. Zhang, *Ceram. Int.* 37 (2011) 1245–1249.
- [4] J.P. Kopasz, J.M. Miller, C.E. Johnson, *J. Nucl. Mater.* 212–215 (1994) 927–931.
- [5] J.D. Lulewicz, N. Roux, *J. Nucl. Mater.* 307–311 (2002) 803–806.
- [6] A. Deptuła, W. Łada, T. Olczak, B. Sartowski, A.G. Chmielewski, C. Alvani, S. Casadio, *Nukleonika* 46 (3) (2001) 95–100.
- [7] C. Alvani, P.L. Carconi, S. Casadio, V. Contini, A. Dibartolomeo, F. Pierdominici, A. Deptuła, S. Lagos, C.A. Nannetti, *J. Nucl. Mater.* 289 (2001) 303–307.
- [8] K. Tsuchiya, H. Kawamura, T. Takayama, S. Kato, *J. Nucl. Mater.* 345 (2005) 239–244.
- [9] K. Tsuchiya, H. Kawamura, M. Nakamichi, H. Imaizumi, M. Saito, T. Kanzawa, M. Nagakura, *J. Nucl. Mater.* 219 (1995) 240–245.
- [10] G. Shanmugavelayutham, V. Selvarajan, *Bull. Mater. Sci.* 27 (5) (2004) 453–457.
- [11] X.L. Jiang, M. Boulos, *Trans. Nonferrous Met. Soc. China* 16 (2006) 13–17.
- [12] O.P. Solonenko, *Thermophys. Aeromech.* 21 (6) (2014) 735–746.
- [13] S.M. Ko, S.M. Koo, W.S. Cho, K.T. Hwang, J.H. Kim, *Ceram. Int.* 38 (2012) 1959–1963.
- [14] S.W. Xue, P. Proulx, M.I. Boulos, *J. Phys. D.* 34 (2001) 1897–1906.
- [15] D. Bernardi, V. Colombo, E. Ghedini, A. Mentrelli, *Pure Appl. Chem* 77 (2) (2005) 359–372.
- [16] J.G. Li, M. Ikeda, R. Ye, Y. Moriyoshi, T. Ishigaki, *J. Phys. D: Appl. Phys.* 40 (2007) 2348–2353.
- [17] H.L. Zhu, H.H. Tong, F.Z. Yang, Q. Wang, C.M. Cheng, *Adv. Mater. Res.* 1058 (2014) 221–225.
- [18] T. Laha, K. Balani, A. Agarwal, S. Patil, S. Seal, *Metall. Mater. Trans. A* 36 (2) (2005) 301–309.
- [19] R. Ramaraghavulu, S. Buddhudu, G.B. Kumar, *Ceram. Int.* 37 (2011) 1245–1249.
- [20] M. Hong, Y.C. Zhang, M.Q. Xiang, Y. Zhang, *J. Nucl. Mater.* 459 (2015) 235–240.
- [21] H.B. Xiong, L.L. Zheng, L. Li, A. Vaidya, *Int. J. Heat Mass Transf.* 48 (2005) 5121–5133.